Single-longitudinal-mode optical parametric oscillator for spectroscopic applications

Mes, J.; Leblans, M.J.R.; Hogervorst, W.

published in
Optics Letters
2002

DOI (link to publisher)
10.1364/OL.27.001442

document version
Publisher's PDF, also known as Version of record

Single-longitudinal-mode optical parametric oscillator for spectroscopic applications

J. Mes, M. Leblans,* and W. Hogervorst

Department of Physics and Astronomy, Laser Centre Vrije Universiteit, De Boelelaan 1081, 1081 HV Amsterdam, The Netherlands

Received March 13, 2002

We have developed a tunable, narrow-bandwidth nanosecond optical parametric oscillator system and applied it to spectroscopic studies. The system consists of a narrow-bandwidth grazing-incidence oscillator and a seeded power oscillator, generating Fourier-transform-limited 1.5-ns pulses (bandwidth <500 MHz) in the wavelength range 435 to 2000 nm with energy of 3.5 mJ at a pump energy of 22 mJ. Continuous scanning over 30 to 100 GHz (depending on wavelength) is demonstrated by recording of the resonance line of the Hg atom at 253.7 nm and a vibrational transition of the CO_2 molecule at 1528 nm.

OCIS codes: 190.4970, 300.6210, 300.6390.

An optical parametric oscillator (OPO) is an attractive, highly efficient solid-state source of coherent radiation tunable over a wide wavelength range.[1] Free-running OPOs, however, exhibit a broad spectral bandwidth that is not desirable for many applications. Several mechanisms for reducing this bandwidth have been explored, including injection seeding with a narrow-bandwidth (diode) laser[2,3] and the use of frequency-selective intracavity elements such as etalons.[4] Several successful attempts to reduce the bandwidth of an OPO with a grating under grazing incidence in the cavity have been reported.[5,6] However, cavity losses are high in such a configuration, and hence the efficiency of these systems is low. Also, these systems exhibit strong output power fluctuations. We have developed a new configuration that is basically a master oscillator power amplifier system. The narrow-bandwidth master oscillator is a grazing-incidence optical parametric oscillator (GIOPO). Its output seeds the power OPO [(POPO) see Fig. 1]. This system provides stable output power in a single longitudinal mode (SLM) with an overall efficiency of 14.5%.

The OPO system is pumped with the third harmonic of a Coherent Infinity Nd:YAG laser. This laser delivers SLM pulses of 3-ns duration at 355 nm at a repetition rate of 1 to 100 Hz, with a top-hat intensity distribution in the relay plane of the laser. This top-hat intensity distribution makes the laser an excellent pump laser for OPOs. To maintain the intensity distribution of the laser beam, we relay image the beam into both OPO cavities, using two telescopes. These telescopes are also used to reduce the beam diameter of the pump laser. The telescope for the GIOPO has a magnification ratio of 2.75:1, and the telescope for the POPO has a ratio of 2.2:1. Both the GIOPO and the POPO are pumped with 11 mJ of power from the Nd:YAG laser at 35 nm.

The GIOPO consists of two uncoated 28° type I β-barium borate (BBO) crystals (10 mm $\times$ 5 mm $\times$ 5 mm) in a walk-off-compensated configuration. The pump light is coupled into the cavity via a flat end mirror that is highly reflective for the signal wave. Behind the crystals, the pump light is coupled out through a dichroic mirror, this prevents grating damage by the pump light. The grating is chosen such that only a first-order reflection can occur. The first-order reflection is retroreflected into the cavity by the tuning mirror. The zero-order reflection of the grating provides the light that is coupled out of the cavity.[7] To improve the efficiency of the GIOPO, which is operated close to threshold, we couple the residual pump light back into the cavity by use of a high-reflecting mirror, and this light is used again in the amplification of the parametric waves.

Three sets of optics and gratings are used to cover the wavelength range from 435 to 2000 nm. A 2400-line/mm grating and a set of high reflectors is used to oscillate signal waves from 465 to 600 nm, with corresponding idler waves in the range 1500 to 1000 nm, and an 1800-line/mm device with a second set of high reflectors covers the signal wavelength range from 600 to 710 nm, with corresponding idler waves ranging from 1000 to 710 nm. The remaining wavelengths, signal waves from 430 to 465 nm and idler waves from 1500 to 2000 nm, are generated by means of resonating the idler wave in the cavity. The reflection efficiency of an infrared-reflecting 750-line/mm grating under grazing-incidence angle is much higher than the reflection of blue light on a 3600-line/mm grating in the same configuration. Since a grating under grazing incidence has low reflection efficiency (<3%),[8] one must operate the GIOPO close to threshold to avoid damage of the BBO

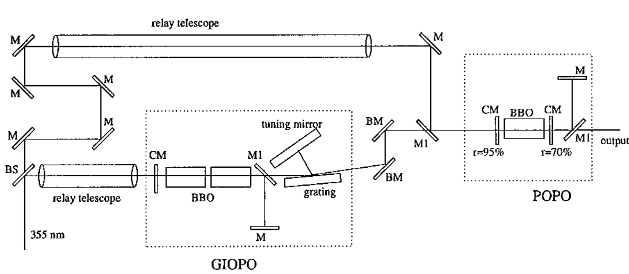

Fig. 1. Experimental setup: M's, high-reflecting mirrors for 355 nm; M1s, mirrors that are highly reflecting for 355 nm and highly transmissive for signal and idler waves; CMs, cavity mirrors, highly reflecting for signal or idler waves and highly transmissive for 355 nm; BMs, bending mirrors, high reflecting for signal or idler waves; BS, 50% beam splitter for 355 nm.

0146-9592/02/161442-03$15.00/0

crystals by high pump intensity. This requirement results in low power output and strong intensity fluctuations. The oscillation threshold of the GIOPO is 8 mJ. The GIOPO delivers 100-μJ pulses of 1.5 ns at 11-mJ pump power. These pulses are further amplified in the POPO. For single-mode operation, the cavity length can be changed by application of a voltage to the piezo on which the end mirror is mounted. Scanning can be achieved by a change in the angle of the tuning mirror with respect to the grating. For this purpose, the tuning mirror is also mounted on a piezo crystal. The scan range is limited to 100 GHz by the maximum expansion of the tuning mirror piezo. For scans of moderate length (<100 GHz), the phase-matching angle of the crystals does not have to be adjusted.

The POPO consists of a BBO crystal (cut at an angle of less than 28° for type I phase matching), 12 mm × 7 mm × 7 mm in size, placed between an input coupler ($R = 95\%$ for signal wavelength, highly transparent for pump and idler waves) and an output coupler ($R = 70\%$ for signal wavelength, highly transparent for pump and idler waves). The cavity length is minimized to 2.5 cm, which corresponds to a free spectral range of 6 GHz. This cavity length is necessary to obtain as many round trips as possible during the temporal width of the pump pulse and thus drive the POPO into saturation. This saturation results in stable output power. Moreover, when the mode spacing in the cavity of the amplifier is large, it is easier to maintain single-mode operation. An advantage of the power oscillator is that it acts as a spectral filter as well, since its free spectral range differs from that of the GIOPO. The GIOPO has a free spectral range of 1.9 GHz, so if multimode operation occurs, the side modes are separated by 1.9 GHz from the main mode. If the POPO is locked on the main mode of the GIOPO, these side modes do not fit into the POPO cavity and will not be amplified (see Fig. 2). The POPO delivers 3-mJ output pulses of 1.5 ns at a pump energy of 11 mJ (efficiency 27%).

Seeding is most efficient when the seed pulse reaches the POPO slightly before the pump pulse. The pump pulse to the POPO is delayed by 1 ns with respect to the seed pulse generated in the GIOPO. The cavity length of the POPO is adjusted with a piezoelectric transducer so that the mode of the GIOPO fits inside the POPO cavity. Hence, the POPO will oscillate on exactly the same wavelength as the GIOPO. The distance between the two oscillators is chosen to be longer than the length of the generated pulse, so that the light generated in the POPO does not disturb the single-mode operation of the GIOPO.

The spectral structure and the relative frequency of the GIOPO and POPO are monitored on a home-built spectrum analyzer that consists of a CCD camera (Pulnix TM6AS) mounted behind a 9-GHz air-spaced Fabry–Perot interferometer. In Fig. 2, typical framegrabber pictures of the mode structure of the GIOPO and the POPO are shown. Single-mode operation of the GIOPO–POPO combination is controlled by this spectrum analyzer and a feedback program written in a combination of the C^{++} and Labview languages.

When the GIOPO is well aligned, it runs more or less in single mode ($\leq$2 small side modes) and the software determines the positions of the peaks of the spectrum analyzer and the center of mass of the peaks belonging to one etalon order. Next, the positions of the side peaks are determined. A suitable voltage for the piezo mounted on the end mirror is calculated to change the cavity length to suppress these side modes. Then, the length of the POPO cavity is adjusted as well so that the mode of the GIOPO matches this length precisely. The spectrum analyzer fringes of the POPO will show up at the same position as those of the GIOPO. Under this condition, the seeding will work efficiently, and the POPO will oscillate on a SLM. However, it is essential that the alignment of the POPO with respect to the spatial distribution of the seed beam and the generated beam is perfect, otherwise single-mode operation cannot be achieved.

The absolute wavelength of the POPO is measured by a wavelength meter (type ATOS Lambdameter LM-007). This wavelength meter consists of a temperature-stabilized monolithic quartz block containing four neon-filled Fizeau interferometers with different free spectral ranges. This system can measure wavelengths from 400 to 1100 nm with an accuracy of 0.003 cm^{-1}. A small fraction (1%) of the light from the GIOPO and the POPO is coupled into single-mode fibers and used for analysis. The light from the POPO is split into two parts, one part for the spectrum analyzer and the other part for the Lambdameter to measure the wavelength of the device. When the measured wavelength is different from the lock wavelength, software calculates the desired shift in the positions of the spectrum analyzer fringes (of the GIOPO and the POPO). From this shift the applied voltage to the different piezos is subsequently calculated. Scanning of the device is achieved in a similar way: The lock wavelength is now shifted step by step under computer control. The wavelength and the Fabry–Perot spectra can be measured only in the visible region because of the coupling fiber used and the etalon coating. To determine the infrared idler wavelengths generated in the OPOs, the software

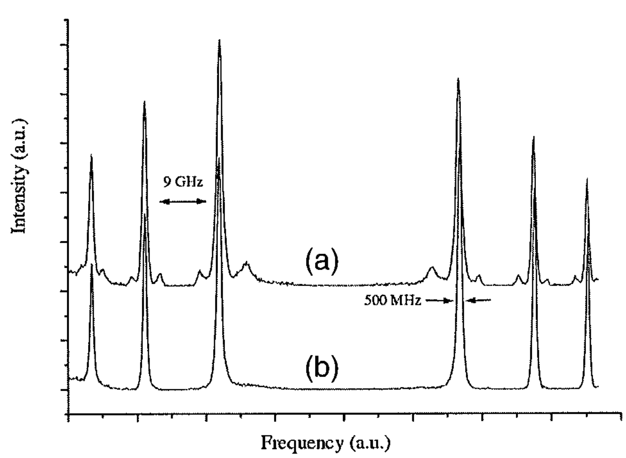

Fig. 2. Fabry–Perot spectra of (a) GIOPO and (b) POPO. The Fabry–Perot interferometer has a free spectral range of 9 GHz and a finesse of 20. The FWHM of the POPO is 500 MHz.

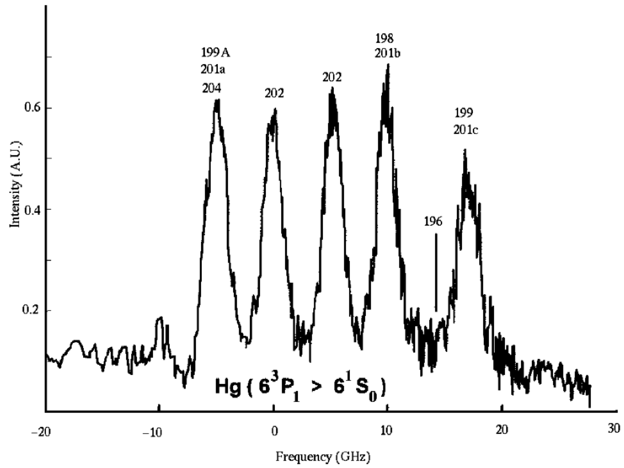

Fig. 3. Absorption spectrum of Hg vapor at 253.7 nm.

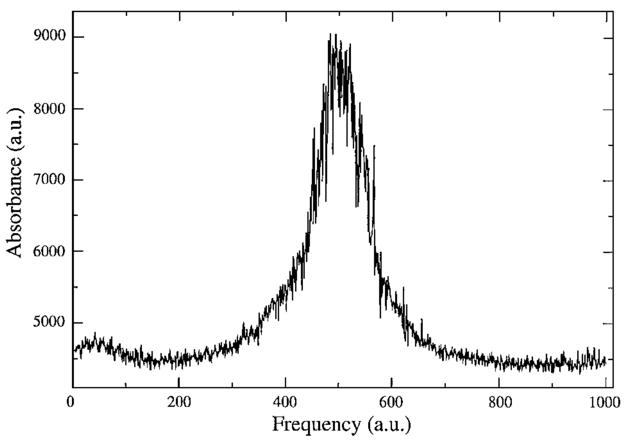

Fig. 4. Cavity ringdown measurement of the 6543.952-cm^{-1} transition of CO_2.

calculates the wavelength of the infrared idler wave from a measurement of the signal wavelength and the wavelength of the second harmonic of the pump laser. From these measurements the wavelength of the third harmonic (the pump wavelength) follows, as does the idler wavelength. The system has high intrinsic stability; without active stabilization the GIOPO–POPO system is single mode for minutes, and the actively stabilized system is single mode and drifts no more than 200 MHz for hours.

The output wavelength range of the system can be further expanded by second-harmonic generation. By collimation of the POPO output into two BBO crystals cut at an angle of less than 55° in a walk-off-compensated setup, for example, 750-μJ ultraviolet light was generated with 3.2 mJ at 474 nm.

This OPO device is a versatile tool for spectroscopic experiments because of its wide wavelength tuning range and narrow bandwidth. This versatility is demonstrated here with two different types of experiment. First, the resonance transition of the Hg atom at 253.7 nm was measured. For the transition from the ground state to the first excited state, the output of the POPO oscillating at 507 nm was frequency doubled, generating wavelengths near 253.7 nm. The Hg was heated in a cell to a pressure of 200 mTorr. A direct absorption experiment was performed. The length of the optical path through the vapor is 1 m. The absorption and intensity fluctuations were measured with two identical photodiodes. The OPO system was scanned over 40 GHz. In Fig. 3, a measured spectrum is shown, and the absorption peaks for the different Hg isotopes are clearly resolved.

To test the capabilities of the OPO device for scanning in the infrared wavelength range, we performed a cavity ringdown absorption experiment[9,10] on CO_2 at 1528 nm. The cavity mirrors used for this experiment have a radius of curvature of 1 m and a reflectivity of 99.99%. The cavity decay transient was detected by a high-speed InGaAs photodiode with a spectral response in the range 800–1800 nm and a rise–fall time of 5 ns. The decay time of the empty cavity was measured to be 7.5 μs. In Fig. 4, a CO_2 absorption line at 6543.952 cm^{-1} is shown; the line was measured at a pressure of 76.1 Torr in the cavity. The absorption cross section of this line is 0.24×10^{-6} atm^{-1} cm^{-2}. On the left-hand side of Fig. 4 another transition (at 6544.075 cm^{-1}) is visible; this line has a strength of 0.15×10^{-6} atm^{-1} cm^{-2}.

In conclusion, we have demonstrated an efficient tunable SLM OPO system that can be electronically scanned over 2.5 cm^{-1}. We can expand this scanning range by mounting the tuning mirror on a piezo stack with a larger expansion or by the use of a picomotor. This device is, as demonstrated, widely applicable in spectroscopy. However, the use of a SLM pump laser is a prerequisite for SLM operation of the OPO system.

The authors thank B. van Oerle and J. Offerein for their assistance with the spectroscopic experiments and acknowledge financial support from the Technologie Stichting STW. J. Mes's e-mail address is mes@nat.vu.nl.

*Present address, Tibotec, Generaal De Wittelaan 11-B3, 2800 Mechelen, Belgium.

References

1. V. G. Dimitriev, G. G. Gurzadyan, and D. N. Nikogosyan, in *Handbook of Nonlinear Optical Crystals*, A. E. Siegman, ed., 3rd rev. ed. (Springer, New York, 1992), p. 345.
2. A. Borsutzky, Quantum Semiclass. Opt. **9,** 191 (1997).
3. J. M. Boon-Engering, W. E. van der Veer, J. W. Gerritsen, E. A. J. M. Bente, and W. Hogervorst, Opt. Lett. **20,** 330 (1995).
4. See the feature on Optical Parametric Devices, J. Opt. Soc. Am. B **12,** 2084–2320 (1995).
5. W. R. Bosenberg and D. R. Guyer, Appl. Phys. Lett. **61,** 387 (1992).
6. L. A. W. Gloster, I. T. McKinnie, Z. X. Jiang and T. King, J. M. Boon-Engering, W. E. van der Veer, and W. Hogervorst, J. Opt. Soc. Am. B **12,** 2117 (1995).
7. M. G. Littman and H. J. Metcalf, Appl. Opt. **17,** 2224 (1978).
8. E. G. Loewen, M. Neviere, and D. Maystre, Appl. Opt. **16,** 2711 (1979).
9. A. O'Keefe and D. A. G. Deacon, Rev. Sci. Instrum. **59,** 2544 (1988).
10. H. Naus, S. J. van der Wiel, and W. Ubachs, J. Mol. Spectrosc. **192,** 162 (1998).